SAND76-8221
Unlimited Release

^{3}He Release From UT_3

K. L. Wilson, M. E. Malinowski, M. I. Baskes

Prepared by Sandia Laboratories, Albuquerque, New Mexico 87115 and Livermore, California 94550 for the United States Energy Research and Development Administration under Contract AT (29-1) 789

Printed July 1976

Sandia Laboratories

SF 2900 Q(7-73)

When printing a copy of any digitized SAND Report, you are required to update the markings to current standards.

Issued by Sandia Laboratories, operated for the United States Energy Research and Development Administration by Sandia Corporation.

NOTICE

This report was prepared as an account of work sponsored by the United States Government. Neither the United States nor the United States Energy Research and Development Administration, nor any of their employees, nor any of their contractors, subcontractors, or their employees, makes any warranty, express or implied, or assumes any legal liability or responsibility for the accuracy, completeness or usefulness of any information, apparatus, product or process disclosed, or represents that its use would not infringe privately owned rights.

SAND76-8221
UNLIMITED RELEASE
July 1976

^{3}He RELEASE FROM UT_3*

K. L. Wilson, M. E. Malinowski, and M. I. Baskes
Sandia Laboratories, Livermore, California 94550

ABSTRACT

Recent Mound Laboratory data for the temperature and particle size dependence of ^{3}He release from UT_3 are summarized. The quasi steady-state ^{3}He early release rate is shown to increase with increasing specific surface area, and the ^{3}He release characteristics are shown to be temperature insensitive near 25°C. A qualitative model for ^{3}He mobility in UT_3 is proposed, and an estimate of the ^{3}He migration energy is made.

*This work is supported by the U. S. Energy Research and Development Administration.

^{3}He RELEASE FROM UT_3

1. Introduction

^{3}He release from UT_3 follows a two-stage release behavior as a function of age. The early release period consists of a small, constant release of ^{3}He; the second stage is accelerated release, characterized by a rapid evolution of ^{3}He after a critical age has been reached. The observed release fraction* is qualitatively depicted in Figure 1. An understanding of the behavior of ^{3}He during the first year is crucial to the development of quantitative models for UT_3. This paper deals with the analysis of recent release data from Mound Laboratory's UT_3 storage program. A qualitative model of ^{3}He mobility in UT_3 is developed, and it is applied to both the early and accelerated release periods.

---

*The release fraction is defined as:

$$\frac{\text{Total } ^3\text{He Released}}{\text{Total } ^3\text{He Generated}} = \frac{\int dt\ (^3\text{He Release Rate})}{\int dt\ (^3\text{He Generation Rate})}$$

The normalized release rate is given by:

$$\frac{^3\text{He Release Rate}}{^3\text{He Generation Rate}}$$

During the early release period of UT_3 a quasi steady-state ^{3}He release develops rapidly after T_2 loading, and:

$$\text{Release Fraction} \simeq \text{Normalized Release Rate}$$

In the accelerated release period, this approximation is not valid.

2. Experimental Results

Mound Laboratory has recently measured the effect of UT_3 surface area on ^3He release.[1] Surface areas were determined by BET* measurements, and ^3He release data were obtained by gas analysis. Figure 2 presents the early release data as a function of initial surface-to-mass ratio for UT_3 powders stored at 25°C with a T_2 overpressure. Each data point is the average ^3He release fraction in a group of sample containers loaded from the same batch of UT_3. The data are derived from measurements of samples between 100 to 200 days old, a time during the early release period. Since specimens are sampled only three to four times each year, the results presented here are the only gas analyses taken during the early release period. However, weekly transducer readings of the total sample pressure indicate that a plateau does exist in the ^3He release rate. The error bars denote the maximum and minimum values of the ^3He release from the samplings. There were four specimens per surface area for the November, 1973, loading, and either one or two specimens per surface area for the October, 1974, loading. Also plotted in Figure 2 are the results of a ^3He surface release model developed in Section 3. The time to accelerated release also depends on surface area, with multiple pass powders achieving accelerated release significantly earlier than single pass powders.

The temperature dependence of ^3He release from UT_3 is also being measured by Mound Laboratory.[1] Table I shows that the early release data from samples stored at -40 to +70°C are comparable to those of similar powder surface areas stored at 25°C. There does not appear to be any large temperature dependence of the early release rate measured in the 100-200

*Brunauer-Emmett-Teller method of surface area determination.

day age period, over the range -40 to +70°C; all samples of a given surface area have reached a temperature independent, quasi steady-state release rate by ∿100 days. The time to accelerated release for the 0.8 m^2 g^{-1} UT_3 powders also does not show any obvious temperature dependence between -40 and +70°C.

3. Discussion

There have been several theories of ^3He release from UT_3. W. D. Wilson first proposed that the formation of ^3He bubbles in the lattice could qualitatively explain the two stage ^3He release. However, this concept was discarded in favor of a model involving percolative coalescence of immobile ^3He atoms.[2] At this same time period, R. Alire fitted the existing ^3He release data with a second order release model.[3] More recently, Bowman and Attalla made NMR measurements of UT_3 powders, and concluded that ^3He bubbles are being formed as early as two months after T_2 loading.[4] R. Alire has also recently developed a ^3He release model involving the growth of bubbles.[3] It is clear that the mobility of ^3He will determine which mechanism is actually operational in UT_3 at ambient temperatures. The recent ^3He release data provide important new information. They show that the early release rate increases with increasing specific surface area, and that ^3He release is temperature insensitive near room temperature.

The following model has been devised to explain the gas release data in the early release period. Isolated ^3He atoms are considered to be mobile at room temperature in the UT_3 lattice. The sink structure for ^3He in a UT_3 particle consists of the free surface of the particle (an external sink) and a distribution of internal sinks such as grain boundaries, inclusions,

^{3}He self-clusters, vacancies and vacancy clusters on the tritium sublattice. (The significantly lower release of ^{3}He from UT_3 stored in vacuum may indicate a sizable vacancy - ^{3}He interaction). The early release rate in this model, which is the ^{3}He current to the external particle surface normalized by the total ^{3}He generation rate, is determined by the competition for the mobile ^{3}He between the external and internal traps.

The simplest model for this physical system makes the following assumptions:

1) The powder consists of uniform spheres of radius r.
2) All ^{3}He born within a shell of material at the surface of thickness Δr is released at the generation rate, and $\Delta r \ll r$.
3) The remaining ^{3}He atoms born in each particle are immediately trapped.

With these assumptions, the steady-state normalized release rate (R) is given by:

$$R = \frac{4\pi r^2(\Delta r)}{\frac{4}{3}\pi r^3} = \frac{3(\Delta r)}{r} \tag{1}$$

The average particle radius (r) can be related to the experimentally determined specific surface area (S) and density (ρ) by

$$r = \frac{3}{\rho} \quad (S)^{-1} \tag{2}$$

Substitution of Eq. (2) into (1) yields:

$$R = \rho(\Delta r)S \tag{3}$$

Equation (3) is plotted in Figure 2, with $\rho = 10\ gcm^{-3}$ and $\Delta r = 50$ Å.

Possible criticisms of this simple model include the facts that the UT_3 particles are not spherical and these particles are not all the same size. For example, Figure 3 is an SEM micrograph of UT_3 with a specific surface area, S of ~3 m^2g^{-1}. The individual particles clearly are not of the same shapes or sizes. In order to help assess the relationship of particle size distribution in the early release as derived above in Eq. (3), assume again a model of UT_3 as spherical particles, but now with a distribution of particle sizes N(r) such that N(r)dr is the number of UT_3 spheres in the range $r \rightarrow r + dr$.

Additionally:

$$\langle r^n \rangle = \int drN(r)r^n / \int drN(r)$$

$$N_t = \int drN(r)$$

Considering again the release from a shell of thickness Δr in the UT_3 spheres, and assuming negligible helium retention in the shells (i.e., helium is released at generation rate), the helium release rate from the spheres is given by :

$$R = \frac{\int drN(r)[r^3 - (r-\Delta r)^3]}{\int drN(r)\ r^3} \tag{4}$$

Since $r^3 - (r-\Delta r)^3 = 3(\Delta r)r^2 - 3(\Delta r)^2 r - (\Delta r)^3$, Equation 4 reduces to:

$$R = \frac{\int drN(r)\ 3(\Delta r)r^2 - \int drN(r)\ 3(\Delta r)^2 - \int drN(r)(\Delta r)^3}{\int drN(r)r^3} \tag{5}$$

Since

$$\frac{\int drN(r)\ r^2}{\int drN(r)\ r^3} = \frac{A\rho}{3M} = \frac{\rho S}{3} \tag{6}$$

with A = Total Surface Area

M = Total Mass

Then

$$R = \rho(\Delta r)S - \frac{3(\Delta r)^2 \langle r\rangle}{\langle r^3\rangle} - \frac{(\Delta r)^3}{\langle r^3\rangle} \tag{7}$$

Thus, to first order in Δr, the magnitude of the early release is identical to that obtained in Eq. 3 and is <u>independent of the particle size distribution</u>. Second order terms in Equation 7 have been evaluated assuming $N(r) = \delta(r-r_o)N_T$ and have been found to be $\lesssim 4\%$ of the first order terms for specific areas of ~3 m^2g^{-1}.

These calculations can be performed assuming cubical UT_3 particle shapes, and a distribution of cube sizes. The results for R are identical to that given in Eq. 3, with r = the cube half-edge. In fact, to first order in Δr, the results of Eq. 3 hold regardless of the particle shape and distributions.

To show this, let N_k = number of UT_3 particles of a shape and size indicated by the index k. Then, to first order in Δr, the release from the shell region is given by

$$R \simeq \frac{\sum_k N_k \int dA_k\ (\Delta r)}{\sum_k N_k \int dV_k} \tag{8}$$

with dA_k = differential area element of particle k,

and dV_k = differential volume element of particle k.

Thus,

$$R \simeq \frac{\rho(\Delta r) \sum_k N_k \int dA_K}{\sum_k N_k \int dV_k \cdot \rho} = \frac{\rho(\Delta r)A}{M} = \rho(\Delta r)S \tag{9}$$

The early release rate is an order of magnitude higher than would be expected of surface release from the first monolayer. The preceding analysis indicates that the rather large shell thickness ($\Delta r \sim 50\text{Å}$) obtained by our analysis of the Mound data is independent of the distribution of particle size or shapes. Physically, the 50 Å shell thickness is an effective diffusion length for internal trapping. Any ^{3}He born deep inside the particle will be internally trapped, while a ^{3}He atom born very near the surface has a very high probability of escaping, and therefore contributing to the early release. The early release rate in this quasi steady-state is determined by geometric considerations of the diffusion lengths to the various sinks.

This model can be made more quantitative by solving the diffusion equations for ^{3}He. The problem of diffusion of a mobile defect in the presence of trapping sites has been studied in detail (see Sosin and Bauer,[5] and Seidman[6]). The equations are:

$$\frac{\partial C_{He}}{\partial t} = D_{He}\nabla^2 C_{He} - \lambda C_{He} + \mu C_s + G \tag{10}$$

$$\frac{\partial C_s}{\partial t} = \lambda C_{He} - \mu C_s \tag{11}$$

where G is the constant generation rate of ^3He, C_{He} is the concentration of mobile ^3He and C_s is the concentration of trapped ^3He. The coefficient λ represents a trapping rate and μ is the detrapping rate; D_{He} is the diffusivity of ^3He in UT_3. It is assumed that the concentration of trapping sites is constant, that the traps are unsaturable and that the detrapping rate is negligibly small. Then the partial differential equations decouple, and one only has to solve:

$$\frac{\partial C_{He}}{\partial t} = D_{He} \nabla^2 C_{He} - \lambda C_{He} + G \tag{12}$$

The coefficients λ and D are given by:

$$\lambda = g_1 C^* \nu e^{(\Delta s/k)} e^{(-\Delta h/kT)} \tag{13}$$

$$D = g_2 a_o^2 \nu e^{(\Delta s/k)} e^{(-\Delta h/kT)} \tag{14}$$

where g_1 and g_2 are geometric factors, C^* is the trap concentration, ν is the vibrational frequency of ^3He in UT_3, a_o is the ^3He jump distance, and Δs and Δh are the entropy and enthalpy of migration of ^3He. Equations (13) and (14) can be rewritten as

$$D = D_o e^{-\Delta h/kT} \tag{15}$$

$$\lambda = \alpha D \tag{16}$$

with

$$\alpha = \frac{g_1 C^*}{g_2 a_o^2} \tag{17}$$

The release rate (R) is given by:

$$R = \frac{3}{Gr} \left(\frac{dC_{He}}{dx}\right)_{x=r} \tag{18}$$

Equation (12) was solved numerically, with a spherical UT_3 particle of radius r and with α and D as parameters. The parameter D was arbitrarily chosen so that a steady state release was achieved by 0.05 years; α was then adjusted so that the steady state release rate was ~16% for r = 1000 Å ($S = 3\ m^2 g^{-1}$). (This choice of α corresponds to a trap concentration of ~10^{-4} atom fraction on the tritium sublattice.) With this choice of D and α, the particle radius (r) was varied, and the results of Eq. 18 are almost identical to those of Eq. 3.

The numerical solution also provides information about the time dependence of the early release rate. Figure 4 shows the effect of varying the ^3He diffusivity with other parameters held constant. For $D < 10^{-19}$ $cm^2\ s^{-1}$ the release rate will not reach a steady state within the first year. For higher diffusivities, the steady state is reached more rapidly, and the steady-state rate is independent of diffusivity. The generation rate of ^3He then becomes the rate limiting step in the release rate. In order to fit the observed release behavior, the diffusivity therefore must be $\gtrsim 10^{-19}$ $cm^2\ s^{-1}$ at -40°C (233K). The diffusivity is related to

temperature by Eq.15; assuming $D_o \simeq 10^{-3}$ cm^2 s^{-1}, then, we require $\Delta h \lesssim 0.7$ eV. As long as this inequality is obeyed, there will be negligible temperature dependence in the early release plateau at all storage temperatures. Below -40°C, however, the diffusivity will eventually reduce to a point where diffusion becomes the rate limiting step in the release; at that temperature a large temperature dependence will develop (e.g., see Figure 4, $D = 10^{-20}$ cm^2 s^{-1}). In addition, the flux to the internal traps and the release at the surface simultaneously reach a temperature independent steady state. Providing that $\Delta h \lesssim 0.7$ eV, ^3He is diffusing fast enough near room temperature so that the generation rate of ^3He also becomes the rate limiting step for accumulation at internal traps.

Up to now, only the early release period has been discussed. However, the model developed in the previous analysis can be extended to the accelerated release phenomenon. Figure 5 schematically shows one possible configuration for a UT_3 particle. The ^3He flux to internal traps leads to the formation of small bubbles. Eventually, a critical pressure or size is reached by the bubbles, and the particles begin to fracture from the internal stress. New, shorter diffusion paths are opened up to the surface; a significantly higher fraction of the particle volume is connected to the external ^3He sink, and the release rate increases rapidly. The time to this accelerated release is the time required for the internal sinks to reach their critical ^3He concentration. As mentioned previously, the ^3He flux to the internal sinks rapidly achieves a temperature independent steady state near room temperature for $\Delta h \lesssim 0.7$ eV. Hence the time to accelerated release is also temperature independent in this model, above -40°C.*

*Percolation theory, with immobile ^3He (i.e., $\Delta h >> 1$ eV), predicts the lack of temperature dependence in the release rate. However, it cannot explain the NMR data indicating bubble formation.[5,6]

For storage temperatures well below this temperature, however, the time to accelerated release should increase, as the ^3He mobility decreases.

In summary, a model has been developed for ^3He release from UT_3, involving a mobile ^3He atom and a competition for the diffusing species between external and internal sinks. The internal sinks are assumed to be a random distribution of unsaturable point traps, and serve as the nucleation sites for ^3He bubble growth. This model predicts that a steady-state, temperature independent, early release rate will develop with time. This early release of ^3He comes primarily from a 50Å thick surface layer. The accelerated release period is assumed to begin when the internal traps achieve a critical ^3He concentration; at that time the UT_3 particles are irreversibly deformed, and new diffusional pathways are opened up. In order to explain the observed lack of temperature dependence in ^3He release from UT_3, the model requires that the enthalpy of migration (Δh) of ^3He in UT_3 is $\lesssim 0.7$ eV.

REFERENCES

1. K. Foster, Private Communication.
2. W. D. Wilson, Private Communication.
3. R. Alire, Private Communication.
4. R. C. Bowman, Jr. and A. Attalla, (Mound Laboratories), "NMR Study of ^{3}He in Uranium Tritides," presented at the March 1975 Meeting of the American Physical Society, Denver, Colorado.
5. A. Sosin and W. Bauer, Phys. Rev. 147 478 (1966).
6. D. N. Seidman, J. Phys. F: Metal Phys. 3, 393 (1973).

TABLE I

Sample Number	Loading Date	Surface Area (m^2 g^{-1})	Storage Temperature (°C)	Age at Sampling (days)	Release Fraction (% of ^3He generated)
SINGLE PASS:					
16	11/11/73	0.6	25	142	5.4
17	11/11/73	0.6	25	142	7.0
18	11/11/73	0.6	25	184	6.8
19	11/11/73	0.6	25	184	5.1
56	10/30/74	0.8	-37	133	2.8
57	10/30/74	0.8	-37	133	3.2
67	10/30/74	0.8	25	131	1.6
68	10/30/74	0.8	25	131	Bad Transducer
65	10/30/74	0.8	70	132	3.4
66	10/30/74	0.8	70	132	3.6
MULTIPLE PASS:					
20	11/12/73	1.5	25	140	15.3
21	11/12/73	1.5	25	140	13.2
22	11/12/73	1.5	25	183	16.6
23	11/12/73	1.5	25	183	14.5
60	10/30/74	2.3	25	131	6.8
61	10/30/74	2.3	25	131	8.9
58	10/30/74	2.3	70	132	9.1
59	10/30/74	2.3	70	132	6.9
24	11/13/73	3.0	25	141	13.8
25	11/13/73	3.0	25	141	21.5
26	11/13/73	3.0	25	182	11.4
27	11/13/73	3.0	25	182	19.6

ACKNOWLEDGMENTS

Special thanks go to K. D. Phipps and K. Foster for allowing the use of their data, and to G. L. Downs for the scanning electron micrograph of the UT_3 powder. We also wish to acknowledge the many useful discussions with W. D. Wilson, R. Alire, and R. C. Bowman, Jr.

FIGURE CAPTIONS

Figure

1 Schematic representation of ^3He release from UT_3, showing the two stages.

2 The steady state early release fraction as a function of specific surface area.

3 Scanning electron micrograph of 3 m^2/g UT_3 powder. The scale marker is 1μm.

4 The calculated time dependence of the ^3He release rate as a function of ^3He diffusivity.

5 Pictorial description of UT_3 particle during both the early and accelerated release periods.

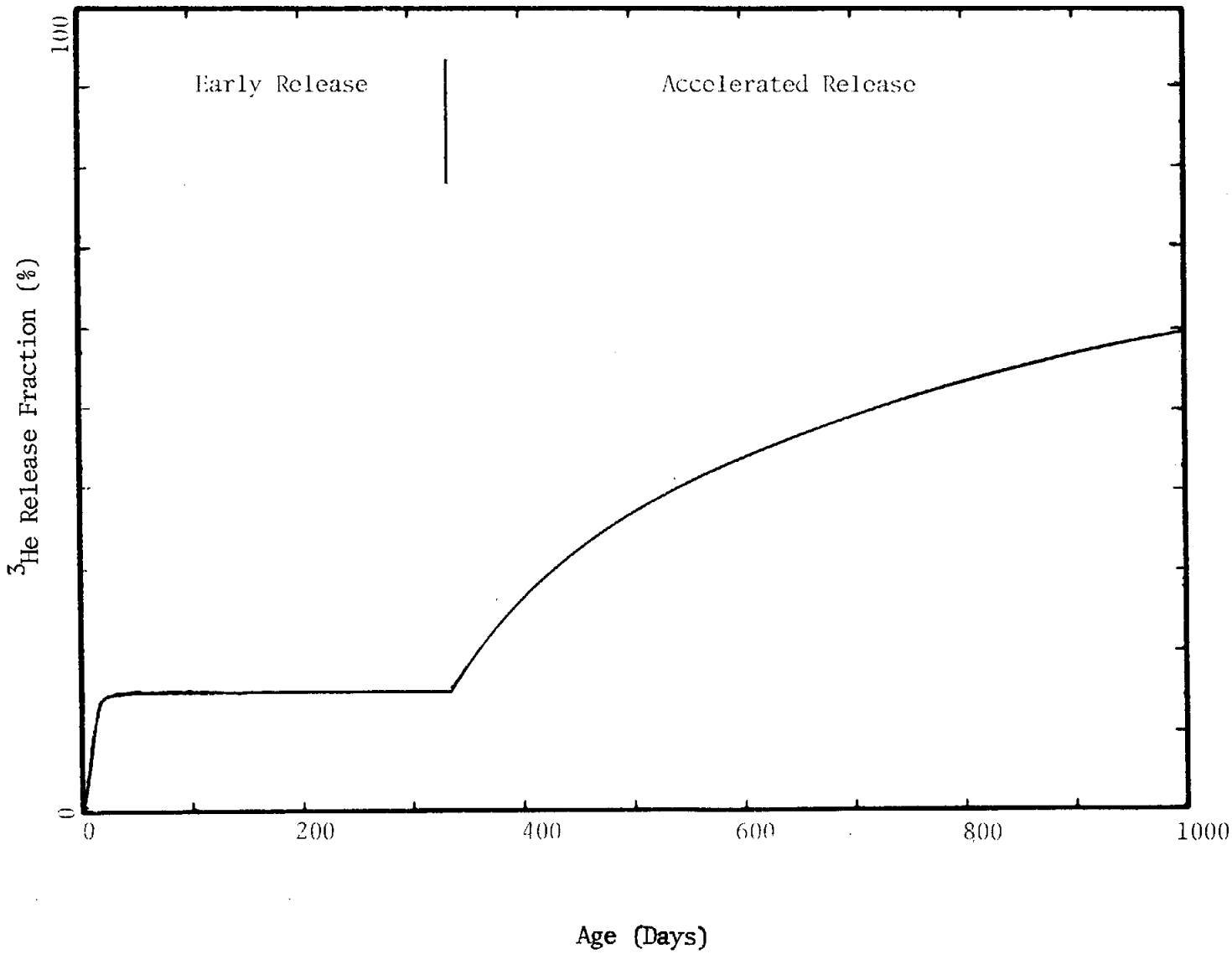

Figure 1: Schematic of ^{3}He Release from UT_3

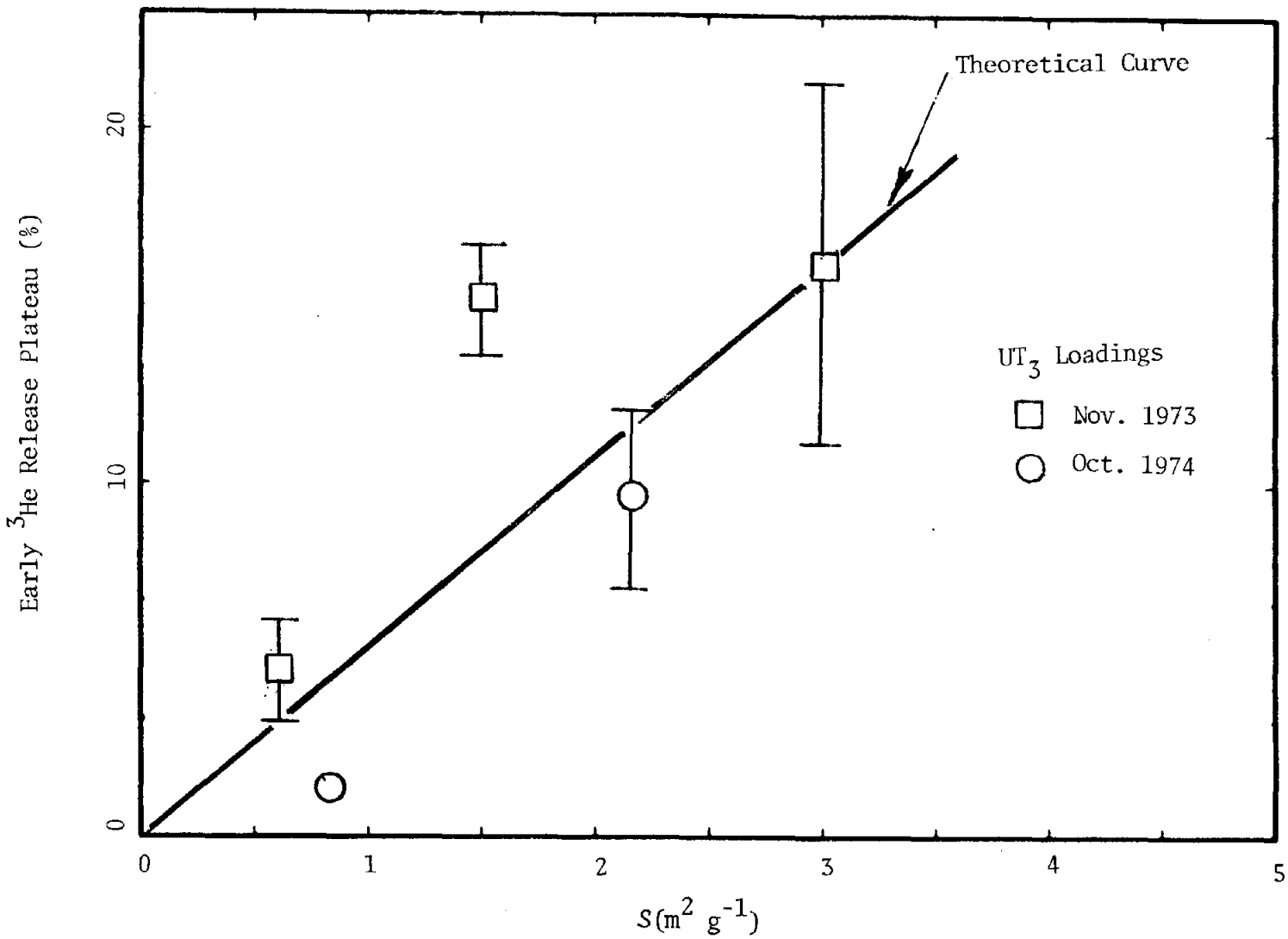

Figure 2: Early ^{3}He Release from UT_3 of Different Surface Areas

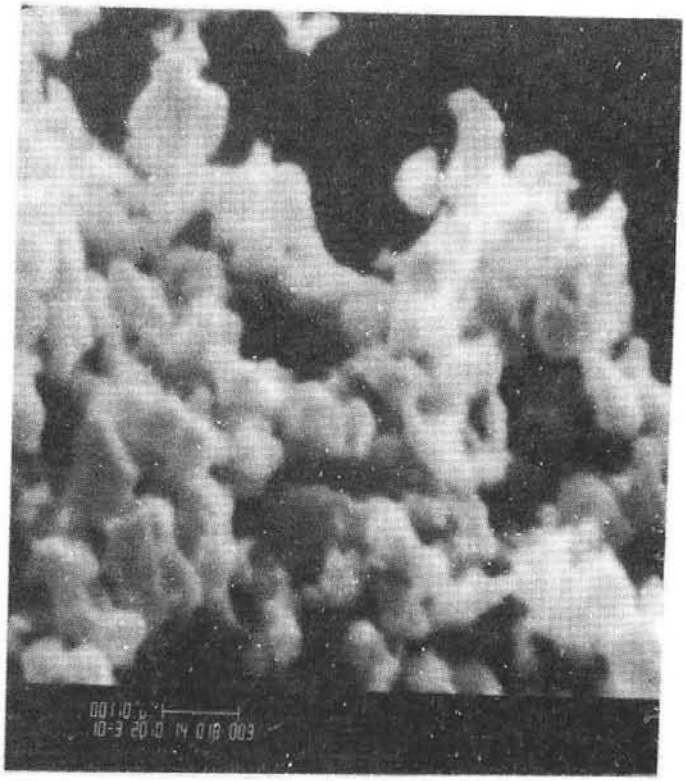

Figure 3: Scanning Electron Micrograph of 3 m^2 g^{-1} UT_3

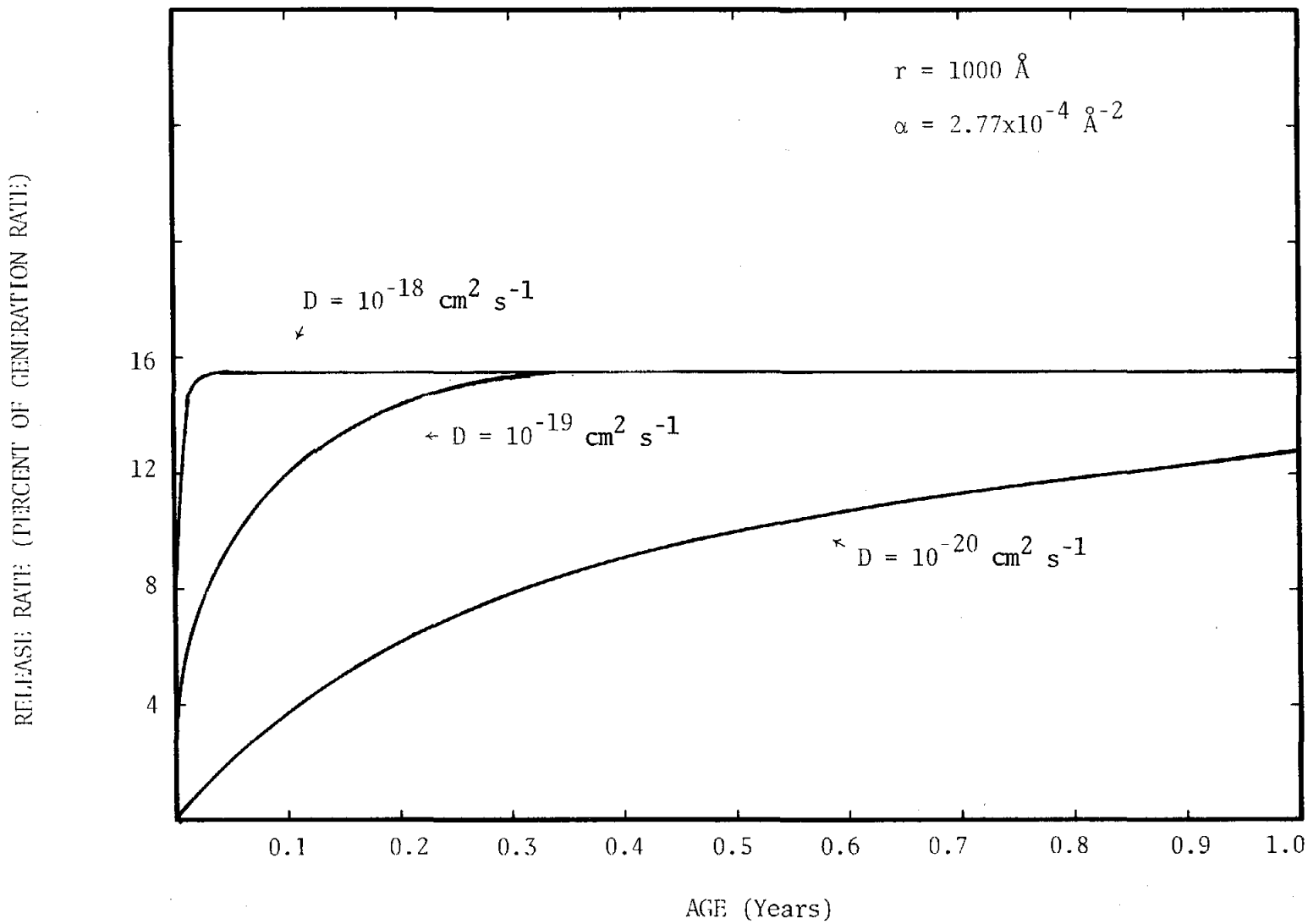

FIGURE 4: Calculated Release Rate for UT_3

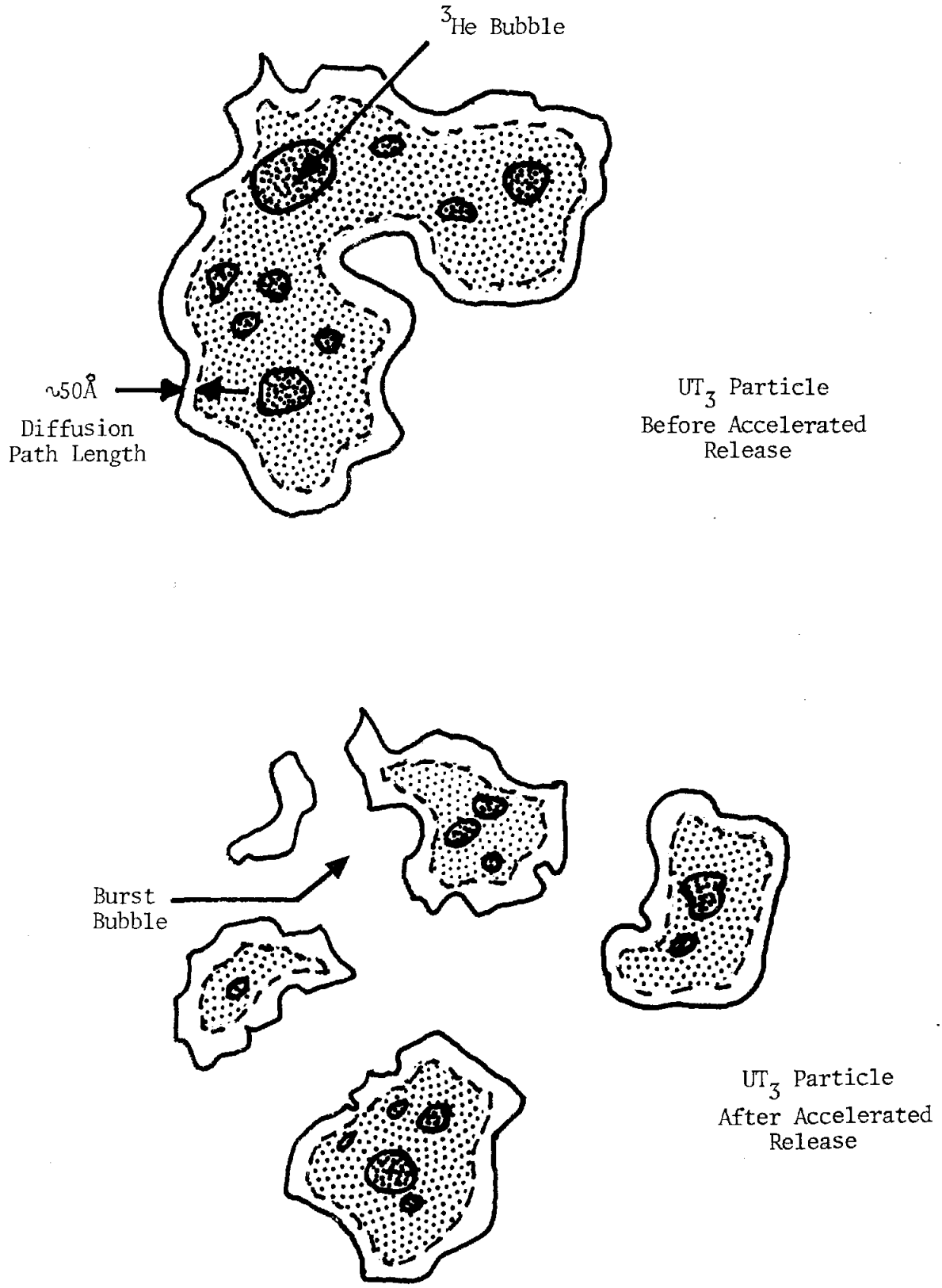

Figure 5: Pictorial Description of UT_3 Particle

UNLIMITED RELEASE

INITIAL DISTRIBUTION

E. I. DuPont de Nemours, Inc.
Savannah River Plant
Document Transfer Section 730-A
Aiken, South Carolina 29801
Attn: J. H. Owen
S. P. Rideout

General Electric Company
Neutron Devices Department
Attn: Document Control
P. O. Box 11508
St. Petersburg, Florida 33733
For: D. H. Ahmann
C. J. Biver
W. C. Brown

Los Alamos Scientific Laboratory
P. O. Box 1663
Los Alamos, New Mexico 87544
For: R. M. Alire
E. H. Eyster
T. E. Larson
E. H. Plassman
R. N. Rogers
T. A. Sanford
J. J. Wechsler

Monsanto Research Corporation
Mound Laboratory
Attn: Records Management
P. O. Box 32
Miamisburg, Ohio 45342
For: H. F. Anderson
R. C. Bowman, Jr.
C. H. Chong
R. J. DeSando
K. W. Foster
C. M. Love
K. D. Phipps
H. L. Turner

Lawrence Livermore Laboratory
P. O. Box 808
Livermore, California 94550
Attn: R. G. Hickman, L-460
H. R. Leider, L-460

DISTRIBUTION (cont'd)

J. C. Crawford, 2350
L. C. Beavis, 2353
W. G. Perkins, 2353
R. S. Blewer, 2353
H. T. Weaver, 2354
F. L. Vook, 5110
J. E. Schirber, 5150
W. J. Camp, 5151

T. B. Cook, Jr., 8000; Attn: L. Gutierrez, 8100
C. H. DeSelm, 8200
W. C. Scrivner, 8400

B. F. Murphey, 8300; Attn: T. S. Gold, 8320
J. L. Wirth, 8340
J. F. Barham, 8360

G. W. Anderson, 8330
J. E. Marion, 8332
L. N. Tallerico, 8332
K. W. Battleson, 8332
M. E. Malinowski, 8334 (25)
W. Bauer, 8334
K. L. Wilson, 8334 (25)
M. I. Baskes, 8341 (25)
W. D. Wilson, 8341

Technical Publications and Art Division, 8265, for TIC (2)
F. J. Cupps, 8265/Library Systems and Technical Processes Division, 3141
Library Systems & Technical Processes Division, 3141 (4)
Library and Security Classification Division, 8266-2 (5)